Active surface and adaptability of fractal membranes and electrodes

Ricardo Gutfraind, Bernard Sapoval

▶ **To cite this version:**

Ricardo Gutfraind, Bernard Sapoval. Active surface and adaptability of fractal membranes and electrodes. Journal de Physique I, 1993, 3 (8), pp.1801-1818. 10.1051/jp1:1993216 . jpa-00246832

HAL Id: jpa-00246832
https://hal.science/jpa-00246832

Submitted on 4 Feb 2008

HAL is a multi-disciplinary open access archive for the deposit and dissemination of scientific research documents, whether they are published or not. The documents may come from teaching and research institutions in France or abroad, or from public or private research centers.

L'archive ouverte pluridisciplinaire **HAL**, est destinée au dépôt et à la diffusion de documents scientifiques de niveau recherche, publiés ou non, émanant des établissements d'enseignement et de recherche français ou étrangers, des laboratoires publics ou privés.

Classification
Physics Abstracts
05.60 — 82.65J

Active surface and adaptability of fractal membranes and electrodes

Ricardo Gutfraind and Bernard Sapoval

Laboratoire de Physique de la Matière Condensée (*), C.N.R.S., Ecole Polytechnique, 91128 Palaiseau, France

(*Received 4 March 1993, accepted in final form 5 April 1993*)

Abstract. — We study the properties of a Laplacian potential around an irregular object of finite surface resistance. This can describe the electrical potential in an irregular electrochemical cell as well as the concentration in a problem of diffusion towards an irregular membrane of finite permeability. We show that using a simple fractal generator one can approximately predict the localization of the active zones of a deterministic fractal electrode of zero resistance. When the surface resistance r_s is finite there exists a crossover length L_c : In pores of sizes smaller than L_c the current is homogeneously distributed. In pores of sizes larger than L_c the same behavior as in the case $r_s = 0$ is observed, namely the current concentrates at the entrance of the pore. From this consideration one can predict the active surface localization in the case of finite r_s. We then introduce a coarse-graining procedure which maps the problem of non-null r_s into that of $r_s = 0$. This permits us to obtain the dependence of the admittance and of the active surface on r_s. Finally, we show that the fractal geometry can be the most efficient for a membrane or electrode that has to work under very variable conditions.

1. Introduction.

Many natural as well as industrial processes take place in the environment of surfaces or at the interface between two media. The surfaces that one encounters in various of these processes are complex and irregular. Examples of natural processes are the exchange of water and inorganic salts between the roots of a tree and its surrounding environment [1] or the transport of oxygen to the blood flow through the surface of the pulmonary alveoli [2]. Among the industrial processes, heterogeneous catalysis and electrochemistry provide the outstanding examples in which porous structures are used to increase the area of exchange and to enhance the global rate [3]. Any process that is limited by transport across a surface or interface can be enhanced using large-surface objects. This is probably the reason why so many natural systems are found that have ramified structures. Many of these surfaces can also be approximately described using fractal geometry [4-7]. Therefore, using the tools provided by the fractal approach can help in analyzing such processes.

(*) Unité de Recherche Associée N° 041254 du Centre National de la Recherche Scientifique.

In the simplest physical situation the mathematical problem is to find the solution of a Laplacian field with mixed boundary condition on the irregular surface. This problem has been first considered in the case of electrochemistry where the Laplacian field is the electric potential in the electrolyte. In electrochemistry, frequency dependent transport experiments can be performed (impedance spectroscopy) which have shown that in the presence of an « irregular electrode » many electrolytic cells have an impedance which behaves as [8-10] :

$$Z_{\text{cell}} = R_b + k(1/r_s + j\gamma\omega)^{-\eta} \tag{1}$$

where R_b can be considered as the bulk or electrolyte resistance, k is a constant, r_s is the Faradaic resistance which describes the finite rate of the electrochemical reaction, γ is the specific capacitance describing the charge accumulation at the surface and η is an exponent which satisfies $0 < \eta \leq 1$. This behavior is known as constant phase angle (CPA). For a smooth electrode $\eta = 1$ and η decreases with the degree of roughness of the electrode. In an electrochemical cell the electrical potential in the electrolyte follows the Laplace equation :

$$\Delta V = 0 \tag{2a}$$

with the boundary condition $V = V_0 \exp(j\omega t)$ on a counter electrode and

$$-\rho^{-1}\nabla V = (r_s^{-1} + j\gamma\omega)V \tag{2b}$$

on the working electrode. Here ρ is the electrolyte resistivity, $\rho^{-1}\nabla V$ is the current density normal to the interface and V is the local potential at some point very near the surface (of the order of the Gouy-Chapman diffusion layer).

It can be shown using linear response theory that a simple and direct connection exists between a.c. and d.c. response [11]. In d.c. conditions the surface contribution to the admittance will be of the form $Y_{\text{surf.}} = k^{-1}(r_s)^{-\eta}$ (the inverse of the second term in equation (1) under d.c. conditions). This is the case we study here. It can be easily shown that this problem can be mapped into that of the response of an irregular membrane or catalyst [12-13]. In the case of a catalytic reaction or transfer across a membrane the Laplacian field is the concentration which satisfies the steady-state diffusion equation $\Delta C = 0$. In a membrane the term r_s is due to the surface resistance which represents the finite permeability through the membrane itself, whereas in a catalyst this term arises from the fact that the probability of the diffusing molecules to have a chemical reaction when they collide with the catalyst surface is less than one (an Eley-Rideal mechanism [14]). Conservation of matter imposes that Fickian transport to the membrane is equal to transport across the membrane. This would be expressed as $-\mathcal{D}\nabla C = WC$ (with $\mathcal{D}$ the diffusion coefficient in the bulk and W the membrane permeability) in exact equivalence with equation (2b).

Many studies, most of them theoretical, have been devoted to this subject and can be found in the literature [11, 15-35]. The goal of this work is not to discuss the different cases which may appear but to concentrate on the case of a wide class of self-similar electrodes. This is the case of 2d electrodes like DLA clusters, diffusion fronts or deterministic fractals as the one shown in figure 1b for which the following result can be written [36, 37] :

$$Y_{\text{surf.}} = (Lb/\rho)(r_s/\rho)^{-(1/D)} L_0^{(1/D)-1} \tag{3}$$

where L is the size of the cell, L_0 is the smallest feature size of the self-similar electrode and b is the thickness of the cell. Thus $\eta = 1/D$, this result has been obtained by three different

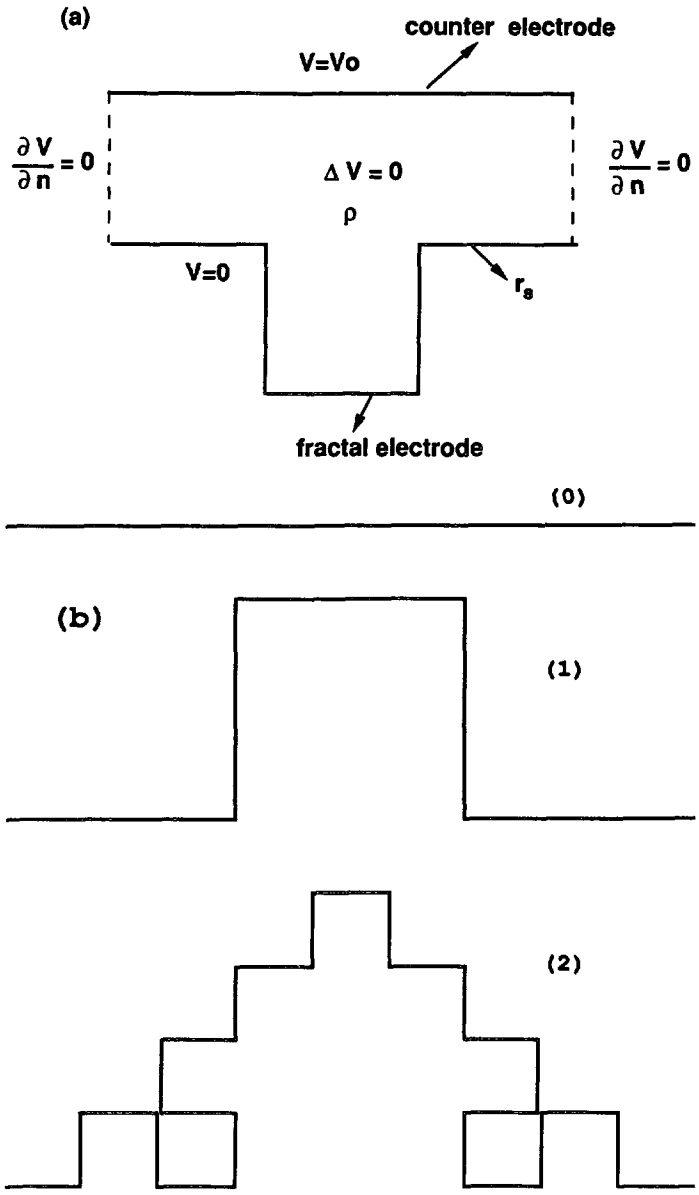

Fig. 1. — a) Schematic representation of the electrolytic cell. The rough electrode is a fractal generator ; b) Generation of a two-recursion level fractal. At each generation the middle third of each segment is substituted by a square ; the fractal dimension is $D = \log (5)/\log (3)$.

methods. First a dimensional analysis with a scaling argument [34], second an iteration method [36, 37] and third extensive numerical simulations based on the exact analogy between electrical and diffusion Laplacian fields [34, 37]. There exist also experiments which confirm this result [37]. It is also convenient to write equation (3) in terms of the admittance Lb/r_s of a flat electrode with the same macroscopic size, and of the characteristic length $\Lambda = r_s/\rho$ [34] :

$$Y_{surf} = (Lb/r_s)(\Lambda/L_0)^{(D-1)/D} \tag{4}$$

The purpose of this paper is to go one step further in the understanding of the process by introducing a simple visual picture of the working regions of a self-similar interface. For this we discuss the concept of an « information set » which is the subset of the surface where the current concentrates [36]. This information set permits a quantitative way to use the concept of growth sites which has been extensively studied in the case of cluster growth problems like D.L.A. [38]. Although this notion is an approximation, it provides a simple way to visualize the active zones of fractal electrodes (and equivalently of membranes and catalysts). This concept permits to find the correct way to renormalize the problem and to obtain equation (3) or (4) through a coarse-graining argument which maps the problem of $r_s \neq 0$ into that of $r_s = 0$. In section 4 we compare the numerical calculations of the current distribution with the geometrical interpretation.

2. Active zone in the case of a Laplacian field around an irregular object.

In this section we propose a practical way of visualizing the regions of an electrode (membrane or catalyst) that can be considered as the active zones for the case $r_s = 0$ (in this case the boundary condition $V = 0$ substitutes the boundary condition (2b) on the fractal electrode). In this situation we search for the regions of the electrode which receive the current (called the information set in Reference [36]).

The information set is a theoretical object on which all the current is supposed to arrive homogeneously. For such a notion to be of any use, it must be compatible with the known macroscopic properties of a two-dimensional Laplacian field : the current concentrates on a subset of the surface whose size scales as L^1, where L is the linear macroscopic size of the object [39]. When the fractal and counter electrode are far away the total current onto the fractal electrode is the same as that measured far away from the surface where the equipotential lines are unperturbed by the surface irregularities. The fractal electrode behaves then as a smooth one and the dimension of the set where the current concentrates has to be one. An intuititive may to understand it is considering that any object in $d = 2$ presents a cross section for random walkers which is proportional to its linear size L [40]. If we construct an information set from a hypothetic « information generator » the construction process must respect this property.

Consider first the problem of the current distribution on the fractal generator shown in figure 1a. If the counter electrode is not too close to the working electrode the potential map for a single pore is expected to behave as shown in figure 2 [41]. In the representation of the

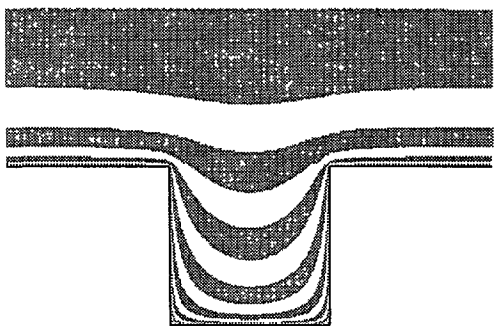

Fig. 2. — Laplacian field around the fractal generator in the case $r_s = 0$ [41]. Each stripe represents a drop in the potential by a factor of 2. The potential $V = 1$ at a distance of the fractal object equal to the width of the central pore.

picture the boundary between the stripes are equipotential lines and the potential varies with a factor two from one line to the next one. The current, by Ohm's law $j = \rho^{-1} \nabla V$, is perpendicular to the equipotential lines and inversely proportional to their separation. One can see that at the entrance of the pore, the density of equipotential lines next to the pore walls is much larger than the density in the central part of the pore. This shows that there is little penetration through the central part of the pore. Therefore, one can see qualitatively that there is a zone of high current (active zone) and a zone of small current.

Based on this and according to the scaling properties that the information set must have (it has to scale as L^1), we construct an information generator, representing the large current zone, as shown in figure 3 (top). (In the language of the multifractal formalism [42] the information set is the set of concentration of the harmonic measure, namely the sites associated with the probability value that dominates the measure.) From the information generator we build the information set by iteration (Fig. 3) but to be consistent with the above requirements, it is necessary for the size of the information generator to be exactly equal to L. This is the only possibility if one wants to build the set from a single generator. If the generator would be equal to $(1 + \alpha) L$, α being any number different from zero, the information set will not scale as L^1 in the iterative process used to build the object. Thus the dashed line in the generator must extend to exactly half of the depth of the well in figure 3 (top).

In summary, if we use the (approximate) notion of an information set, for this notion to be consistent with the known properties of the Laplacian field, the size of the information

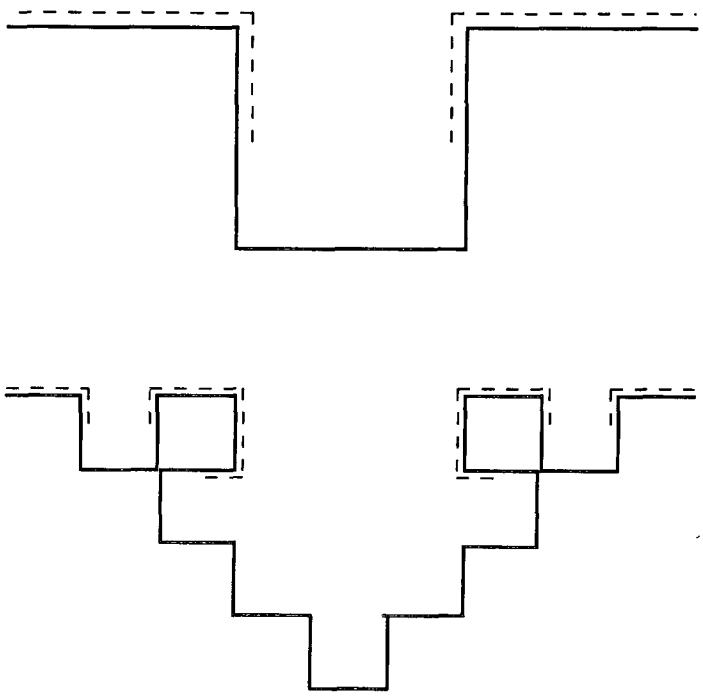

Fig. 3. — Iterative process for the generation of the information set or theoretical active surface. The solid line is the fractal object, the dashed line is its associated information set. At each recursion level each segment is substituted by a version of the generator (top figure) rescaled by a factor $(1/3)^n$, where n is the recursion level. This process assures that independently of the surface irregularities the total length of the information set is the linear size of the object.

generator has to be taken equal to L. The idea of an information set is approximative in two aspects : first not all the current arrives in this fraction of the surface and second the current is not homogeneously distributed on it. However, it is a good approximation when one calculates the exponents that describe the behavior of the system as it is shown in section 3 and 4.

3. Scaling argument.

3.1 SCALING FORM OF THE SURFACE CONTRIBUTION TO THE TOTAL RESISTANCE. — In this section we present a new scaling argument which permits to obtain equation (3). This argument is based on a coarse — graining procedure which maps the problem with boundary condition (2b) on the above situation with $r_s = 0$.

For a real system with finite ρ and r_s the first problem is to compare the surface resistance $R_{surf.}$ with the resistance to access the surface R_{acc}. For very large values of the faradaic resistance r_s, the resistance in the electrolyte becomes negligible in comparison to the resistance of the surface. In this case, there exists an equipotential line that follows the entire surface which can then be considered as exposed to the same potential. The total resistance, which is determined only by the surface contribution, is then proportional to r_s and inversely proportional to the total area of the fractal surface :

$$R_{surf.} = r_s / [b (L/L_0)^D L_0] \ . \tag{5}$$

For a two-dimensional system, independently of the system size, the access resistance is of the order :

$$R_{acc.} \approx \rho / b \ . \tag{6}$$

For given values of ρ and r_s and when $r_s/L_0 > \rho/b$, namely the resistance of the smallest feature of the fractal is larger than the access resistance, the geometrical features can be separated depending on their size : Small parts have a surface resistance larger than the resistance to access them, whereas large features have a negligible surface resistance. Consequently, there

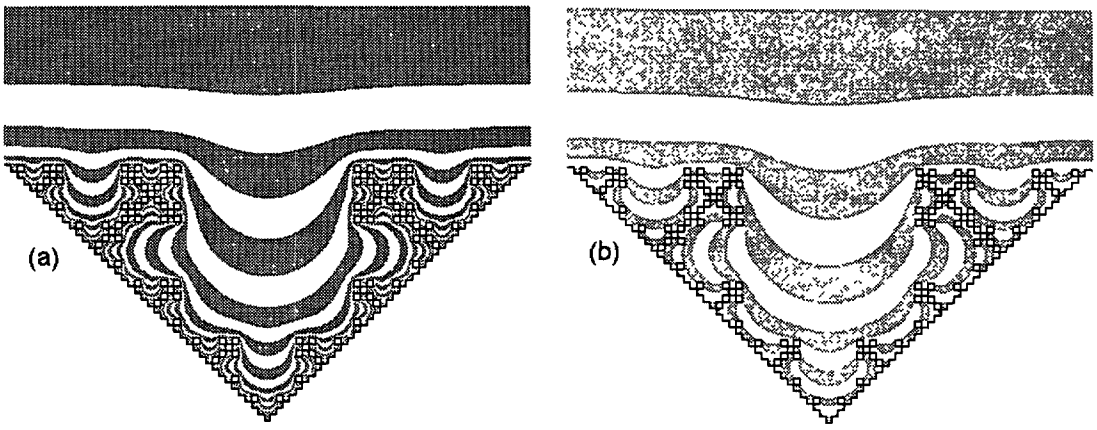

Fig. 4. — The Laplacian potential around a four-iteration object : a) zero faradaic resistance and b) for $\Lambda/L_0 = 3$. The smallest pores are covered only by one stripe. In these pores the surface resistance is larger than the resistance to access to the pore walls. They are approximated as exposed to a constant potential. In the largest pores the access resistance is much larger than the wall resistance and the potential map practically recovers the behavior of $r_s = 0$ (see (a)), the only difference is a local effect near the walls.

exists a crossover length, $L_c(\Lambda)$, which separates two different geometrical behaviors : a) In pores smaller than $L_c(\Lambda)$, the resistance is dominated by the surface and the pore walls can be approximated as exposed to the same potential ; b) In pores larger than $L_c(\Lambda)$ the system recovers the behavior of $r_s = 0$ because the surface impedance is smaller than the access resistance in the electrolyte (see Fig. 4). Then the crossover length is determined by the equality between the surface resistance (Eq. (5)) and the access resistance (Eq. (6)) :

$$r_s / [b(L_c/L_0)^D L_0] \approx \rho/b \tag{7a}$$

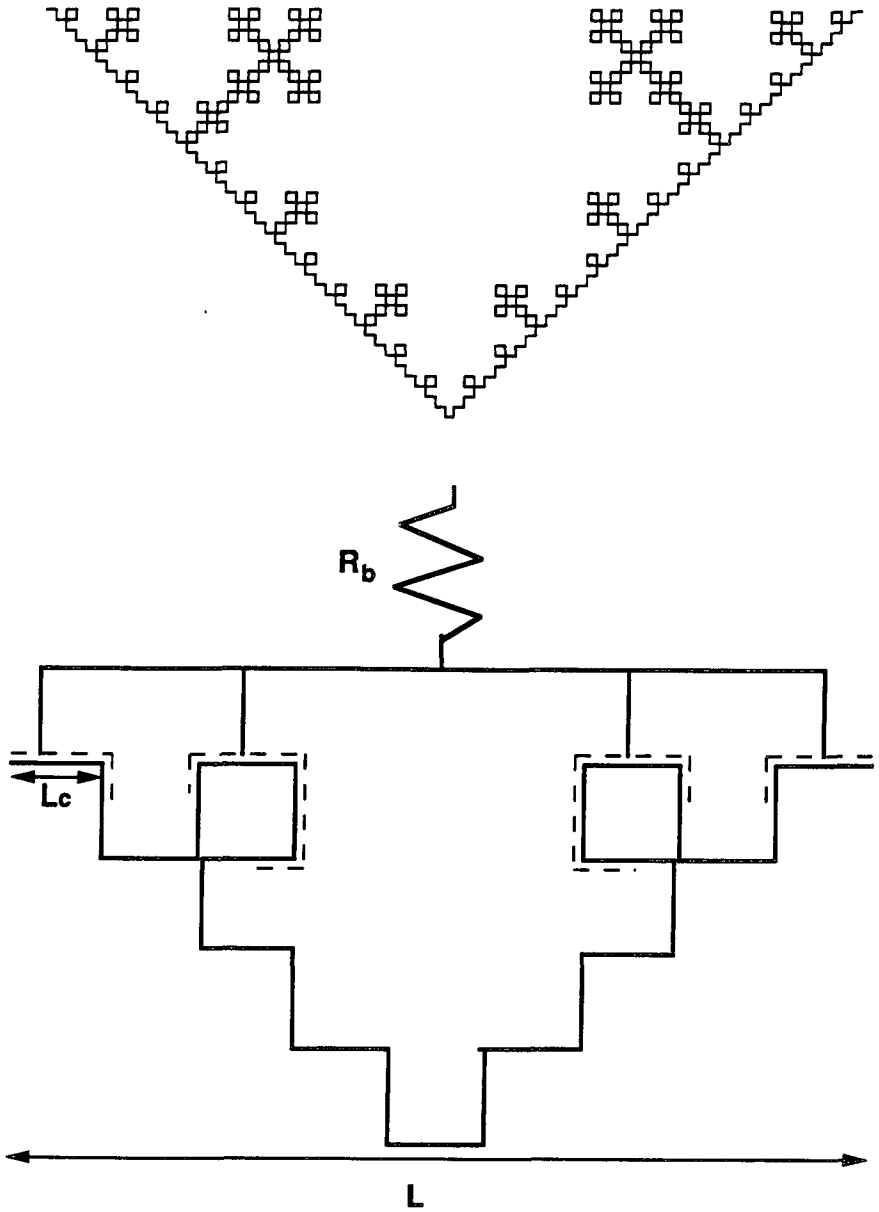

Fig. 5. — A three-iteration object (top) is coarse-grained using the characteristic length shown in the figure. In the coarse-grained object (bottom) the active surface recovers the behavior of $r_s = 0$, namely its total length is L.

or

$$L_c(\Lambda) \approx L_0(\Lambda/L_0)^{1/D} \tag{7b}$$

This means that if one considers a coarse graining of the initial electrode to the size $L_c(\Lambda)$ (see Fig. 5), any larger feature will behave with a surface resistance small as compared to the access resistance ρ/b. Once the object is coarse grained to a new one where the size of the elementary unit is L_c, the resistance of the generated macrosites is small as compared to the access resistance and then the Laplacian field recovers the behavior of $r_s = 0$.
This implies the existence of an active surface of the linear size of the object L (Sect. 2). The difference now is that the bulk resistance R_b (Eq. (1)) is in series with a contribution of the surface. The surface contribution to the admittance is then equivalent to $(L/L_c(\Lambda))$ elements of order (b/ρ) or

$$Y_{surf} \approx (b/\rho)(L/L_c(\Lambda)) \tag{8}$$

which is equivalent to equation (3) or (4). Notice that the coarse graining does not affect the geometry of the cell (the height-length relation), so the bulk resistance (R_b in Eq. (1)), being independent of the surface irregularities, will be the same in both the original and the coarse-grained object.

We would like to point out that the scaling argument developed in this section is general, it is based on the *existence* of an information set of dimension one, but this does not have to be exactly located as it was shown in section 2. However, the iterative procedure that we proposed allows to visualize this set in a very simple manner.

3.2 ACTIVE SURFACE AND ADAPTABILITY. — The scaling form dependence of the active surface on the faradaic resistance, r_s, can also be estimated using the preceeding argument. For a given value of Λ, the surface which corresponds to each macrosite is Λ itself and the number of these macrosites is of the order $L/L_c(\Lambda)$. The total surface of the electrode is $S_T = L_0(L/L_0)^D$ so that the fraction of active surface S_A/S_T is :

$$S_A/S_T \approx (L/L_0)^{1-D} (\Lambda/L_0)^{(D-1)D} \tag{9}$$

An important property arises from the physical picture developed in this section : This is how the fractal surface adapts to environment conditions. One can easily see that this is because the fractal symmetry provides new « active surface » when r_s (or Λ) increases and this part compensates for the larger faradaic resistance.

We recall that the problem of the electrode can be mapped into that of molecules diffusing towards a rough membrane having finite permeability. Then a fractal membrane has the capability of providing new « active surface » whenever it has to absorb molecules having a lower permeability constant, avoiding in part a reduction in the transfer rate. This property can be crucial in the life of many natural systems, where a rough membrane can provide a solution to keep a suitable supply rate for nutrients being in a broad range of permeability values.

4. Numerical results.

4.1 TEST ON A DETERMINISTIC FRACTAL. — In this section numerical results are compared to the theoretical predictions of the previous sections : We have first checked that our numerical calculation of the response agrees with relation (3). To verify that the response of the studied object behaves according to equation (3), we used a relaxation method (see Appendix) to numerically compute the response of an electrochemical cell with a five-iteration object of the

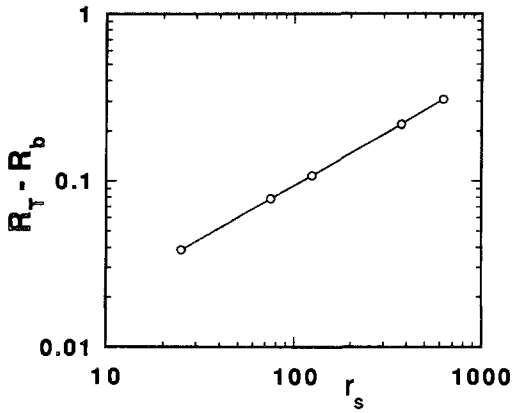

Fig. 6. — Dependence of $(R_T - R_b)$, in computer units, on the faradaic resistance r_s for a five-iteration fractal object of the type shown in figure 1b. $\eta = 0.64$ is obtained from the slope in good agreement with $\eta = 1/D = 0.68$.

type shown in figure 1b. In this calculation one obtains the response of the total electrochemical cell R_T which is the sum of the impedance of the electrode and of the resistance of the bulk of the electrolyte R_b (Eq. (1) under d.c. conditions). The resistance of the electrolyte R_b is the resistance R_T ($r_s = 0$). The exponent η is then obtained from the slope of the log-log plot of $[(R_T - R_T(r_s = 0))]$ against r_s. The value $\eta = 0.64$ is obtained in good agreement with the value $\eta = 1/D = 0.68$ as shown in figure 6 ; the same result was obtained for several other fractal objects [34].

We then test the idea of the information set as an approximation of the active zone in the case $r_s = 0$, by comparing its theoretical localization with actual numerical observations of the active zone of the electrode. Being the information set, as defined in section 2, a simplified active surface, the first thing one can ask is what is the fraction of the total current that indeed reaches it. When $r_s = 0$ the S_A/S_T ratio is equal to $(L/L_0)^{1-D}$. In the case of a five-iteration object of the type shown in figures 1-3 $S_A/S_T = 7.8$ %. From the solution of Laplace equation the current that arrives in each surface site is computed. For comparison purposes one can look at the 7.8 % of the surface associated with the largest local current values. We find first that 86 % of the current arrives in this fraction of the surface. Second, the localization of these sites, as shown by the black points in figure 7, is close to that predicted from the concept of an

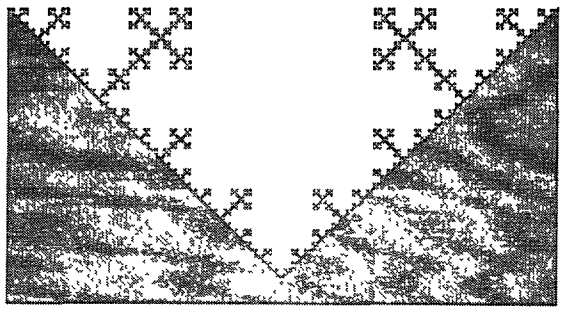

Fig. 7. — Numerical estimation of the active surface ($r_s = 0$) for a five-iteration object (the active sites are in black). The linear size of the object is $L = 729$ lattice units. The active surface are the $L = 729$ boundary sites associated with the largest values of current *per site* ; 86 % of the total current really arrives in this zone. Notice that the part of the surface considered as active is approximately one half of the pore width at each pore wall.

information set as suggested in figure 3. Notice then that the simple procedure suggested in section 2 for generating an information set gives a good approximation of the localization of the most active zones of the fractal electrode.

The information set was defined in section 2 as a theoretical active surface, where the whole current concentrates and where it is supposed to be homogeneously distributed. In fact, the current is not homogeneously distributed in this zone and we now discuss the real current distribution. From the numerical solution of Laplace equation one can classify the surface sites according to the value of current *per site* (j_0). One can then plot $n(j_0)j_0$ *versus* j_0, where $n(j_0)$ is the number of sites associated to a given j_0. This is shown in figure 8 for the case of a five-iteration object. The form of the observed peak indicates that the current concentrates in a narrow band of j_0 values. The surface sites associated to these j_0 values constitute the information set. It is the fact that there exists a narrow peak which permits to approximate the system as if the whole current concentrates in a subset of the surface associated to one value of j_0. This was found to be a good approximation when one calculates the scaling exponents that describe the distribution of current (see for instance Ref. [42]).

We present now the visualization of the working regions of the electrode for different values of the surface resistance [or $\Lambda = r_s/\rho$]. To build the active surface we take the sites associated to the largest j_0 values up to the accumulation of a given percentage of the total current. The case of 86 % of the current for $\Lambda/L_0 = 5$ is shown in figure 9a. One can distinguish two classes of pores, those that behave homogeneously (a continuous line of active zone extends to the bottom of the pores) and those in which the behavior characteristic of $r_s = 0$ is recovered (the active zone penetrates one half of the pore width). It is on this fact that is based the idea of the coarse-graining procedure : The existence of a crossover length upon which one can coarse-grain the object (Fig. 9b) and recover the behavior of $r_s = 0$.

The case of $\Lambda/L_0 = 25$ is shown in figure 10. The picture shows again where arrives 86 % of the total current associated with the largest j_0 values. The same type of behavior as in the case $\Lambda/L_0 = 5$ is observed, but with an increase of the crossover length. Comparing figure 9 and figure 10, one can see that the visual crossover length has been shifted approximately by the factor $(\Lambda_1/\Lambda_2)^{1/D} = (25/5)^{1/D} = 3$ as predicted by equation (7).

According to the theoretical development of section 3, one expects also the scaling relation (9) to be valid. This idea was tested as follows : the active surface is considered as the number of surface sites needed to accumulate a given fraction of the total current (e.g. the black sites in figures 9 and 10 are those needed to get 86 % of the current). Then one can plot the

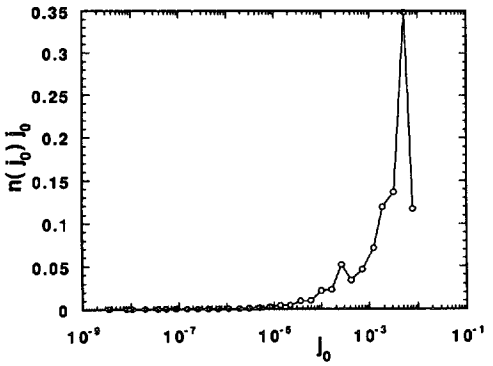

Fig. 8. — $n(j_0)j_0$ *versus* j_0 for a five-iteration object in the case $r_s = 0$.

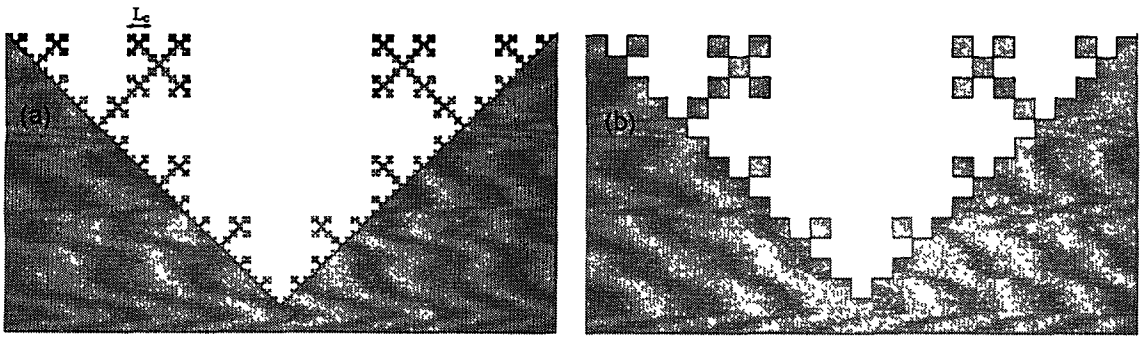

Fig. 9. — Numerical estimations of the active surface for a five-iteration object when $\Lambda/L_0 = 5$. a) In the original object and b) in the coarse-grained object. Notice that the localization of the active surface in the coarse-grained object is close to its theoretical localization.

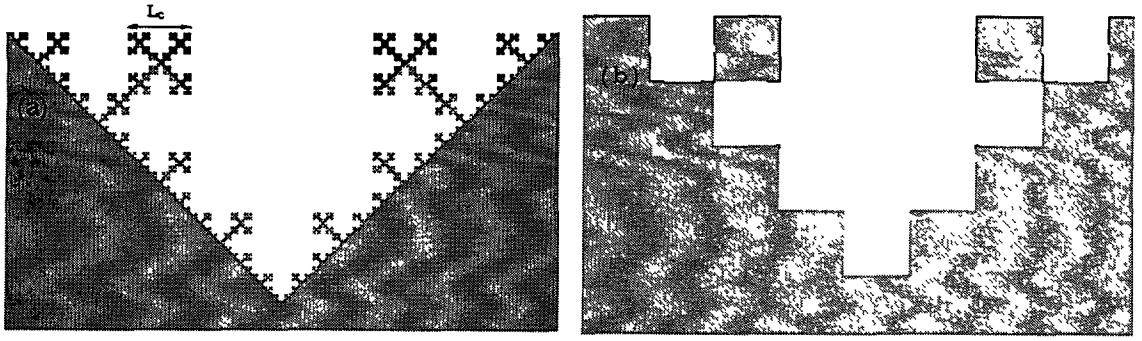

Fig. 10. — Numerical estimations of the active surface for a five-iteration object when $\Lambda/L_0 = 25$. a) In the original object and b) in the coarse-grained object. Notice that there is a shift in the value of L_c by approximately a factor of three with respect to that of figure 9, in agreement with equation (7).

S_A/S_T ratio as a function of Λ. The plots for 75 % and 86 % of the current are shown in figures 11a and 11b respectively. From the slope one gets respectively 0.32 and 0.29, close to the expected value $(D - 1)/D = 0.32$. This shows then that the scaling argument remains true upon changing the selected fraction as far as this fraction remains large.

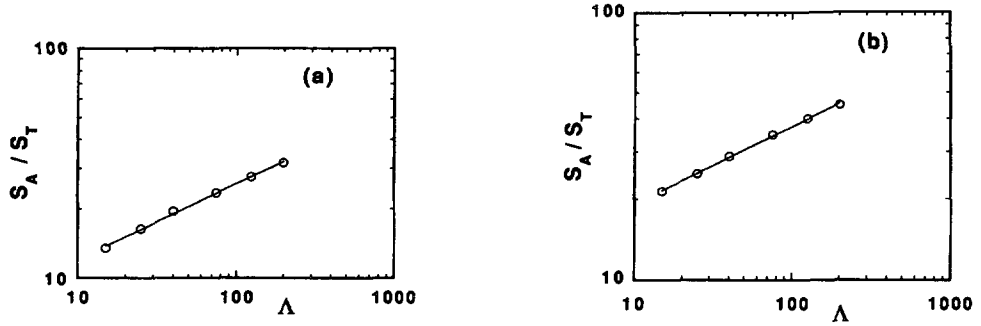

Fig. 11. — Active surface *versus* Λ for a five-iteration object. The active surface is considered the fraction of the surface associated to the largest current *per site* values up to the accumulation of a given percentage of the current : a) the active surface is the fraction of surface required to get 75 % of the total current and b) is the case for 86 % of the total current. A slope equal to 0.32 and 0.29 are obtained in a) and b) respectively, to be compared with the expected value $(D - 1)/D = 0.32$.

4.2 GENERAL PROCEDURE FOR ESTIMATING THE ACTIVE SURFACE IN THE CASE OF RANDOM SURFACES. — In this section we show how the active surface can be determined in the case of random fractal surfaces and suggest a general procedure valid in the case of fractal and non fractal objects. The model of random surface we use is a diffusion front (shown in Fig. 12, for details see Ref. [43]). This diffusion front is built as follows : A source of particles is kept at constant concentration $p = 1$. The particles diffuse (they can jump with probability equal $1/z$ to each of its z neighboring sites under the condition the neighboring site is unoccupied). After a given time a diffusion front is observed, which can be defined as the external frontier of the largest cluster of particles. In fact only part of the frontier is « accessible » to random walkers. This accessible front is the limit of the grey zone in figure 12 and has a fractal dimension $D = 4/3$ [44].

A duffusion front of lateral size $L = 600$ lattice units is the fractal electrode, the counter electrode is located at 100 lattice units from it. We solve the Laplace equation for several values of the faradaic resistance r_s and we verify that equation (1) is satisfied. The value $\eta = 0.75 \pm 0.01$ is obtained, in good agreement with the expected value $\eta = 1/D = 3/4$ (see Fig. 13).

As we did in the previous section we estimate the fraction of the total current which arrives in the theoretical active surface. For the case $r_s = 0$, the S_A/S_T ratio is the linear size of the object L divided by the total length and its value is 17 % : 82 % of the current arrives in this fraction of the surface which is located as indicated in figure 12 by the black sites.

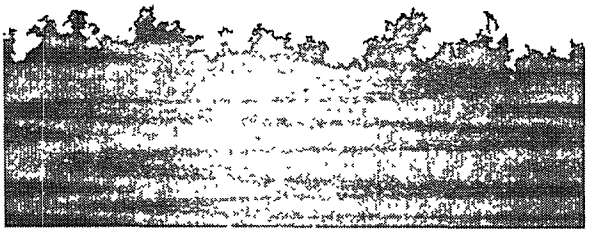

Fig. 12. — Numerical estimation of the active surface. The working electrode is the « accessible » diffusion front of linear size $L = 600$ lattice units. For $r_s = 0$ the active surface is the 600 boundary sites associated with largest j_0 values (black sites). 82 % of the current really arrives in this part of the surface.

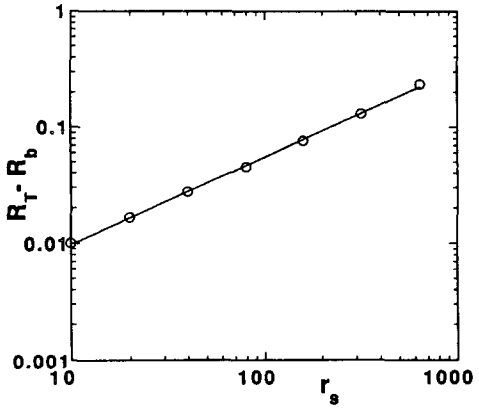

Fig. 13. — $(R_T - R_b)$ as a function of r_s for a diffusion front electrode. A slope equal to 0.75 is obtained, in good agreement with the expected value $\eta = 1/D = 3/4$.

We now discuss about the procedure to localize the active surface for values of the faradaic resistance r_s different of zero. It has been shown that in the equivalent problem of diffusion on a lattice Λ can be defined as a/σ [33, 34], where a is the random walk step and σ is the sticking probability. Λ is of the order of the number of surface sites visited by a walker before being absorbed. Then, zones including a number of sites of order Λ can be considered as perfect absorbents, namely a walker that hits the surface for the first time within this zone is finally absorbed in it. Then the procedure to estimate the active surface can be generalized as follows (applicable to fractal and non-fractal surfaces) : a) The surface is coarse grained in a manner in which each one of the new generated macrosites includes a surface Λ of the *original object*. Notice that for a fractal object the macrosite size will be $L \approx (\Lambda/L_0)^{1/D} L_0$. However, for non-fractal objects the linear size of the macrosites depends on the local irregularity and may be very different in different zones of the surface ; b) On the coarse-grained object the Laplace field behaves as in the case of $r_s = 0$, then once the object is coarse grained, the total length of the active surface is the linear size of the object.

We solve the Laplace equation on the coarse-grained object using the boundary condition $r_s = 0$ on the fractal electrode (in this object the S_A/S_T ratio is the linear size of the object divided by the total surface). We look for the sites of largest j_0 values up to the accumulation of a fraction of surface equal to the known S_A/S_T ratio. We then determine the fraction of the current that arrives in this part of the surface.

We present here the results for two values of Λ. After coarse-graining S_A/S_T is respectively 35 % and 51 % corresponding to $\Lambda/L_0 = 10$ and $\Lambda/L_0 = 40$. The current that arrives in this zone is found to be approximately 84 % for both cases. The slightly larger current fraction obtained in this cases compared with the case $r_s = 0$ is expected to be due to the fact that the coarse-graining diminishes the « losses » of current in the fjords of the irregularities that have been coarse-grained. The localization of these sites are shown in figures 14 and 15 (sites in black).

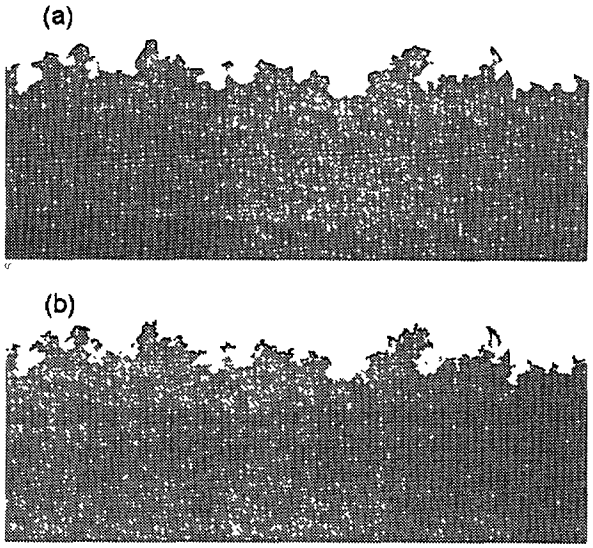

Fig. 14. — Numerical estimation of the active part of the diffusion front surface for $\Lambda/L_0 = 10$. a) The coarse-grained object. Each macrosite corresponds to a zone of the original object that had a surface equal to Λ. The active surface size is the linear measured size of the object : 35 % of the total area and where 84 % of the current arrives ; b) Active surface computed on the original object. In this case 82.5 % of the current arrives in the 35 % of the surface associated with the largest j_0 values, i.e. the active surface. Note that the localization of this zone is approximately the same in both cases.

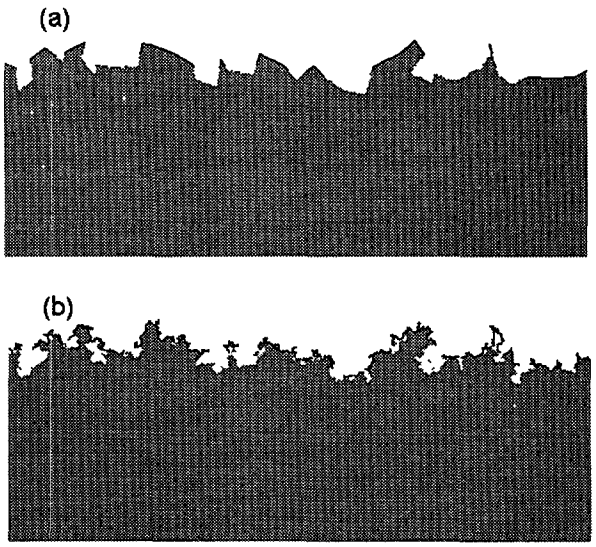

Fig. 15. — a) Numerical estimation of the active surface of the diffusion front for $\Lambda/L_0 = 40$. a) The coarse-grained object. The active surface is in this case 51 % of the total area and where 84 % of the current reaches ; b) Active surface calculated on the original object : 83.5 % of the current arrives in the 51 % of the surface associated with the largest j_0 values. The localization of this zone is approximately the same in both cases.

We compare these results with the numerical solutions in the original object (before coarse-graining) using the surface resistance corresponding to $\Lambda/L_0 = 10$ and $\Lambda/L_0 = 40$ as boundary condition. We look for the current that arrives in the theoretical active surface (35 % for $\Lambda/L_0 = 10$ and 51 % for $\Lambda/L_0 = 40$, see above). For $\Lambda/L_0 = 10$ we find that approximately 85.5 % of the current arrives in this part of the surface, whereas 83.5 % when $\Lambda/L_0 = 40$. These are very closed to what we found for the coarse-grained object. Moreover, the localization of these sites on the surface shows no significant difference with their localization when the system was solved using the coarse-grained object as can be seen comparing (a) and (b) in figures 14 and 15. This procedure permits then to determine the active surface of a membrane, catalyst or electrode on a coarse-grained object instead of the original one, reducing then considerably the time to perform the numerical calculation.

5. Conclusions.

We have shown that the concept of information set or active surface can be a powerful tool in the study of the macroscopic behavior of a Laplacian field around an irregular object. It gives first a very simple picture of the working regions of a fractal electrode or membrane in the case $r_s = 0$. Then a simple coarse-graining procedure permits to find the active surface when $r_s = 0$. This procedure provides a simple visualization of the process and a simple explanation of the transfer equation (3). We have also shown that a fractal membrane is « self-adapted » to variable working conditions. We think that a fractal membrane may be the optimal solution to keep a suitable rate of transfer for absorbing simultaneously molecules having different permeability values. This property can be crucial in the life of many natural systems, where a surface showing irregularities at all length scales can provide sufficient surface for the transfer

at an adequate rate of all the nutrients necessary for the metabolism. We then mentioned that the procedure used to estimate the active surface can be extended to the case of irregular but non-fractal surfaces, which may constitute a powerful tool to study processes of this type in the environment of irregular objects.

Acknowledgments.

We thank M. Rosso for a critical reading of the manuscript and constructive suggestions. We also thank V. Fleury for valuable discussions during this work.

Appendix. Numerical algorithm for the solution of Laplace equation.

To calculate the current onto the fractal surface we solved the Laplace equation (Eq. (2)) using a relaxation method. The discretization of the Laplace equation in the bulk yields :

$$V_{ij} = \frac{(V_{i-1,j} + V_{i+1,j} + V_{i,j-1} + V_{i,j+1})}{4} \tag{A.1}$$

The discretization of the boundary condition equation (2b) for a boundary site (i, j) is given by :

$$\frac{V_{ij} - V_s}{\rho} = \frac{V_s}{r_s/L_0} \tag{A.2}$$

where V_s can be supposed to be the potential at a point very near the surface on the bulk side. So, boundary sites are connected to the surface through a resistance constituted by the bulk resistance ρ in series with the specific surface resistance, r_s/L_0 (see Fig. A.1a). This renders,

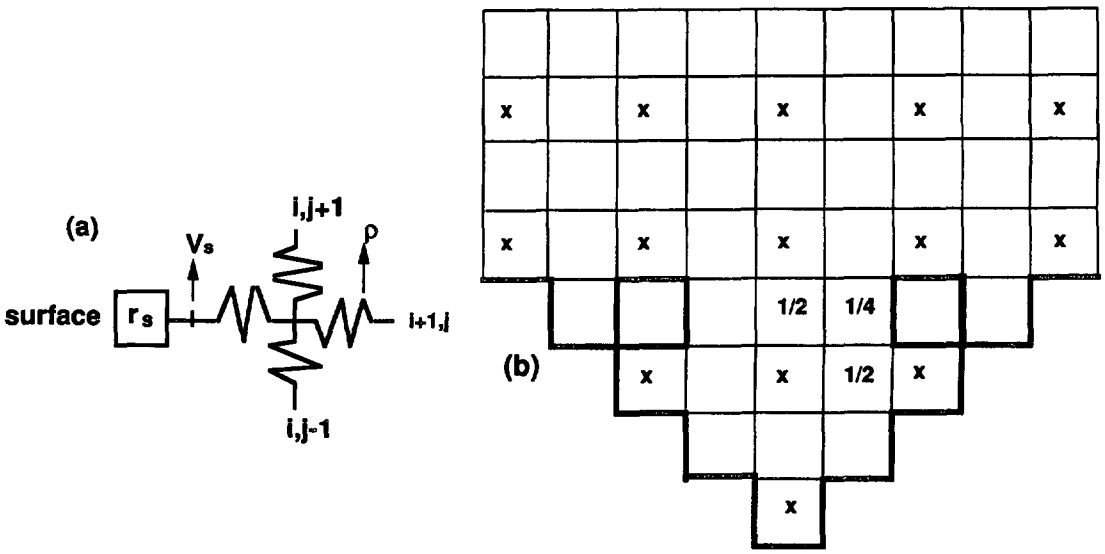

Fig. A.1. — a) Electrical equivalent circuit showing the connection of a boundary site (i, j) with its neighboring sites in the lattice. This is for the case of a boundary site that is next neighbor of only one surface site ; b) Schematic representation of the mesh used in the numerical solution. Sites denoted as « x » are those whose potentials are calculated in the coarse mesh approximation. Those denoted as « 1/2 » are calculated as average of two sites of weight of 1/2 when the interpolation formula is applied, whereas those denoted as « 1/4 » are estimated in the interpolation formula as average of 4 sites of weight 1/4. The fine mesh in the second step is applied only inside the pore structure.

for the case of a boundary site which is next neighbor of only one surface site ($V_{i-1,j}$ is the one substituted by a surface site in Fig. A.1a) :

$$V_{ij} = \frac{(V_{i+1,j} + V_{i,j-1} + V_{i,j+1})}{\left[\dfrac{3+\rho}{r_s/L_0 + \rho}\right]} \tag{A.3}$$

This can be easily extended to the case of boundary sites that are next neighbor of more than one surface site.

We now give some details of the numerical procedure. The mesh size is 1/3 of the unit site used to build the fractal. To accelerate the numerical algorithm, we first solved in a coarse mesh (of grid size 2 × 2 lattice units) and then use the obtained potential values as first input in the second step. In the coarse mesh solution, only the potentials in the sites $V_{2i,2j}$ are calculated (those denoted as (x) in figure A.1b). In the second step we introduced a mesh of two grid sizes, a fine mesh (mesh : 1 × 1 lattice units) inside the pore structure, whereas outside the pore structure the coarse mesh (2 × 2 lattice units) is kept. To obtain the potential values in the sites different from $(2i, 2j)$ in the fine-mesh zone of the two-grid solution (in order to use them as first input in the second step of the solution) the following interpolation formula is applied [45] :

$$\begin{bmatrix} \frac{1}{4} & \frac{1}{2} & \frac{1}{4} \\ \frac{1}{2} & 1 & \frac{1}{2} \\ \frac{1}{4} & \frac{1}{2} & \frac{1}{4} \end{bmatrix}$$

The matrix indicates the weights in the interpolation formula for the calculation of the element $[i, j]$ (the central one in the matrix) of all its neighbors. Then, the weight of i, j itself is 1, that of the sites of type $[(i-1, j) ; (i+1, j) ; (i, j-1) ; (i, j+1)]$ is 1/2 and those of the type $[(i\text{-}1, j-1) ; (i\text{-}1, j+1) ; (i+1, j-1) ; (i+1, j+1)]$ is 1/4. For applying this formula the potential values in the sites that have not been calculated in the coarse mesh approximation [other than those of type $(2i, 2j)$] are zero. Then, in the case of a site of type $2i, 2j$ one recovers the coarse mesh value (all the other eight neighbors have not been calculated in the coarse-mesh approximation and the have zero potentials). The site denoted as 1/2 in figure A.1b will be obtained as average of two sites of weight 1/2, whereas that denoted as 1/4 will be obtained as average of 4 sites of weight 1/4. In the case of boundary sites, the boundary conditions have to be introduced in the interpolation formula.

The approximation of using a mesh of two grid sizes was compared to the results obtained using a fine mesh in the entire lattice. The two-grid solution was found to be much more efficient than a one-grid solution and with almost no effect on the precision. It diminishes the time required to get convergence in 4 or 5 times, depending on the value of r_s, and with an error less than 5/10 000 when the current values are compared to those obtained using a fine-mesh in the entire lattice. It has to be pointed out that in our case the convergence was tested in the total current values and not in the local ones.

References

[1] Hallé F., Oldeman R. A. A., Tomlinson P., Tropical Trees and Forests (Springer-Verlag, New York, 1978).

[2] a) Weibel E. R., The Pathway for Oxygen (Harvard University Press, Cambridge Massachusetts, 1984) ; b) Weibel E. R., Respiratory Physiology, an Analytical Approach, H. K. Chang, M. Paiva Eds. (Dekker, Basel, 1989) p. 1.

[3] a) Aris R., The mathematical theory of diffusion and reaction in permeable catalysts, vol. 1 (Clarendon Press, Oxford, 1975) ; b) Bond G. C., *Surf. Sci.* **156** (1985) 966 ; c) Boudart M., *Adv. Catal.* **20** (1969) 153.

[4] Mandelbrot B. B., Fractal Geometry of Nature, 3rd ed. (Freeman, New York, 1983).

[5] Sapoval B., Fractals (Aditech, Paris, 1990).

[6] a) The Fractal Approach to Heterogeneous Chemistry : Surfaces, Colloids, Polymers, D. Avnir Ed. (Wiley, Chichester, 1989) ; b) For a recent review in catalysis see : Avnir D., Farin D., Pfeifer P., *New J Chem.* **16** (1992) 439.

[7] Feder J., Fractals (Plenum, New York, 1988).

[8] Scheider W., *J. Phys. Chem.* **79** (1975) 127.

[9] Armstrong D., Burnham R. A., *J. Electroanal. Chem.* **72** (1976) 257.

[10] Rammelt U., Reinhard G., *Electrochim. Acta* **35** (1990) 1045.

[11] Sapoval B., Chazalviel J. N., Peyrière J., *Phys. Rev. A* **38** (1988) 5867 and references therein.

[12] Sapoval B., *Acta Stereologica* **6/III** (1987) 785.

[13] Sapoval B., « Fractal electrodes, fractal membranes and fractal catalysts » in Fractals and disordered systems, A. Bunde, S. Havlin Eds. (Springer-Verlag, Heidelberg, 1991) p. 207.

[14] a) Bond G. C., Catalysis by Metals (Academic, New York, 1962) ; b) Adamson A. W., Physical Chemistry of Surfaces, 5th ed. (Wiley, New York, 1990).

[15] Le Méhauté A., *Electrochim. Acta* **34** (1983) 591 and references therein.

[16] Liu S. H., *Phys. Rev. Lett.* **55** (1985) 529.

[17] Kaplan T., Gray L. J. and Liu S. H., *Phys. Rev. B* **35** (1987) 5379 and references therein.

[18] Hill R. M. and Dissado L. A., *Solid State Ionics* **26** (1988) 295.

[19] Ball R., Blunt M., *J. Phys. A : Math. Gen.* **21** (1988) 197.

[20] Blunt M., *J. Phys. A : Math. Gen.* **21** (1989) 179.

[21] Chu Y. T., *Solid State Ionics* **26** (1988) 299.

[22] de Levie R., *Electrochim. Acta* **35** (1990) 1045 and references therein.

[23] Blender R., Dietrich W., Kirchoff T., Sapoval B., *J. Phys. A : Math. Gen.* **23** (1990) 1225.

[24] Geertsma W., Gols J. E., Pietronero L., *Physica A* **158** (1989) 691.

[25] Halsey T. C., Liebig M., *Europhys. Lett.* **14** (1991) 815 and *Phys. Rev. A* **43** (1991) 7087.

[26] Keddam M. and Takenouti H., *C. R. Acad. Sci. Paris Ser. II* **302** (1986) 281 ; Ext. Abstr. 40th I.S.E. Meeting (Kyoto, Sept. 1989) and *Electrochim. Acta* **33** (1988) 445.

[27] Nyikos L. and Pajkossy T., *Electrochim. Acta* **35** (1990) 1547 and references therein.

[28] Marvin M., Toigo F. and Maritan A., *Surf. Sci.* **211/212** (1989) 422.

[29] Mulder W. H. and Sluyters J. H., *Electrochim. Acta* **303** (1987) 303.

[30] Wang J. C., *J. Electrochem. Soc.* **134** (1988) 1915 and *Solid State Ionics* **28/30** (1988) 133.

[31] Bates J. B., Chu Y. T., Stribling W. T., *Phys. Rev. Lett.* **60** (1988) 627.

[32] Kahanda G.L.M.K.S., Tomkiewicz M., *J. Electrochem. Soc.* **137** (1990) 3423.

[33] Sapoval B., *J. Electrochem. Soc.* **137** (1990) 144C and Extended Abstracts, Spring Meeting of the Electrochemical Society, Vol. 90(1) (Montreal, Canada, 1990) p. 772.

[34] Meakin P., Sapoval B., *Phys. Rev. A* **43** (1991) 2993.

[35] Ball R., to be published in Surface Disordering, Growth, Roughening and Phase Transitions, R. Julien, J. Kertesz, P. Meakin, D. Wolf Eds. (Nova Science Publisher, 1993).

[36] a) Sapoval B. and Gutfraind R., Workshop on Surface Disordering, Growth, Roughening and Phase Transitions (Les Houches, April 1992) R. Julien, J. Kertesz, P. Meakin, D. Wolf Eds. (Nova Science Publisher, 1993, p. 285) ; b) Sapoval B., Spring meeting of the Electrochemical Society St. Louis, Missouri, Vol. 92(1) (1992) p. 514.

[37] Sapoval B., Gutfraind R., Meakin P., Keddam M., Takenouti H., *Phys. Rev. E*, accepted.
[38] Evertsz C., Mandelbrot B. B., *Europhys. Lett.* **15** (1991) 245.
[39] Jones P., Wolff T., *Acta Math.* **161** (1988) 131.
[40] There exist certain cases where this exponent is different from one like the Sierpenski electrode analysed in reference [11] but these electrodes present a non homogeneous surface and do not belong to the type of problem analysed here.
[41] Evertsz C., Mandelbrot B. B., Normant F., *J. Phys. A : Math. Gen.* (1992) 1781.
[42] Halsey T. C., Jensen M. H., Kadanoff L. P., Procaccia I., Shraiman B. I., *Phys. Rev. A.* **33** (1986) 1141.
[43] Sapoval B., Rosso M., Gouyet J. F., Ch. 3.2.3 in reference 6.
[44] Grossman T., Aharony A., *J. Phys. A.* **19** (1986) L745 ; ibid. **20** (1987) L1193 ; Meakin P., Family F., *Phys. Rev. A* **34** (1986) 2558.
[45] Stüben K., Trottenberg U., Multigrid Methods, W. Hackbusch, U. Trottenberg, Eds. (Springer-Verlag, Berlin Heidelberg, 1982) p. 1.